Effect of Lead Intoxication on the Postnatal Growth of the Rat Nervous System*

by Martin R. Krigman† and Edward L. Hogan‡

Lead encephalopathy was induced in developing Long-Evans rats by adding lead carbonate (4% w/w) to the diet of nursing mother immediately after delivery. The morphological and biochemical features of cerebral ontogenesis were studied in 30-day-old rats.

By the 30th postnatal day, the overall effect of lead intoxication was retardation of brain growth. The mass of both the cerebral gray and white matter was appreciably reduced in the lead rats without any reduction in cell populations. While the neuronal population was preserved, the growth of neurons was reduced and their maturation retarded. The retarded neuronal growth was characterized by the limited proliferation of processes in the neuropil and by the reduction in the number of synapses per neuron. However, synaptogenesis was neither delayed nor perturbed but reduced by the limited development of neuronal dendritic fields. The myelination was altered and its cerebral content significantly reduced. The effect of lead on myelination was one of hypomyelination. The hypomyelination appears to be primarily related to retarded growth and maturation of the neuron and is not a reflection of a defect in the myelinating glia or a delay in the initiation of myelination.

Introduction

The vulnerability of the nervous system to the toxic effects of lead is most evident in the young. While the neural aspects of plumbism have been the subject of numerous studies, we still have much to learn about the extent of the effects of lead on the nervous system. This is particularly true for body lead burdens in children which have been previously considered nontoxic (*1*, *2*). The nervous system of the young is obviously different from that of the adult. The episodic nature of the growth and maturation of the developing nervous system may make the young more vulnerable at selected periods (*3*) to a hostile environment than the adult.

In an attempt to define the effects of lead on the developing nervous system, we have studied the model of lead encephalopathy

†Department of Pathology, University of North Carolina School of Medicine, Chapel Hill, North Carolina 27514.

‡Department of Medicine (Neurology), University of North Carolina School of Medicine, Chapel Hill, North Carolina 27514. Present address: Department of Neurology, Medical College of South Carolina, Charleston, South Carolina 29401.

*Studies supported by U.S. Public Health Service Grant ES-00481.

described by Pentschew and Garro (*4*). The model uses the nursing rat and is characterized by selected morphological features resembling those of clinical encephalopathy. This report is based upon quantitative morphometric and biochemical analyses of postnatal brain development and contains our findings on the effects of lead on neuronal growth and maturation, synaptogenesis, and myelination. The studies reported herein were limited to the 30th postnatal day. By this time the nervous system is highly developed: the brain weight is nearly three-fourths that of an adult (*5*), neurogenesis has stopped (*5, 6*), synaptogenesis has nearly ceased (*7, 8*), and the most active period of myelination is over (*3*); also, the pups are already weaned.

Materials and Methods

A more detailed description of the animal model, morphometric procedures, and chemical analyses appears in our earlier reports (*9, 10*).

Animal Model

Lead intoxication was produced in the Long-Evans strain of rats by the procedure described by Pentschew and Garro (*4*). Immediately after birth, the lead litters were reduced to six pups per dam, and the nursing mother was given free access to water and a lead-containing diet. This diet was ground Purina Lab Chow to which 4% lead carbonate by weight was added. After weaning at day 25, the lead pups received the same diet as their mothers. The control litters were adjusted to eight pups per litter and the maternal diet was free of lead.

Morphometric Procedures

The morphometric studies of myelin were carried out on three control and three lead rats. Brains were fixed by perfusion with 5% gluteraldehyde in 0.1*M* phosphate buffer, pH 7.4. The pyramids with the corticospinal tracts were isolated from the medulla at the level of the obex. The isolated pyramidal sections were post-fixed in 1% osmium tetroxide in the phosphate buffer, stained *en bloc* with uranyl acetate, dehydrated initially in graded alcohols and finally in propylene oxide, and embedded in Araldite. The specimens were so embedded that the cut sections were perpendicular to the tracts. "Thin" gray sections were cut, and the contrast was enhanced by staining with urany acetate and Reynolds lead citrate stain. A JEOLCO 100–B electron microscope was used in all the studies. A random selection of fields was obtained; the plate magnification was X13,000 and this was enlarged threefold in printing. A calibration picture was taken at each sitting and this never varied more than 3%. The actual morphometric analyses of myelin were carried out upon these calibrated electron photomicrographs. These myelin studies included counts of myelinated and nonmyelinated fibers, measurement of axon size (circumference), and counts of the number of myelin lamellae per axon. From these studies, the percent age of myelinated fibers, the ratio between axon circumference and number of myelinated lamellae, and mean width of myelin lamellae were calculated. The significance of the findings was determined by the appropriate statistical test (*11*).

The morphometric studies of the cortex were carried out on four control and four lead-intoxicated 30-day-old rats. Each of the rats was from a different litter. The brains were fixed by perfusion as described above. The fixed brains were cut, and a coronal section 1 cm thick was removed starting at the level of the origin of the middle cerebral artery. From a given coronal section, two 1-mm wedges of somatosensory cerebral cortex were dissected from each cerebral hemisphere starting at a point 6 mm lateral to the interhemispheric fissure. This procedure yielded four full cortical wedges of somatosensory parietal cortex, area 3 of Krieg (*12*). The cortical wedges were prepared for ultramicrotomy as above. "Thick" 0.5 μ Araldite sections of the full cortical mantle were cut and stained with Toluidine blue. The Araldite blocks were further trim-

med to the molecular layer or cortical layer I and cut and stained for electron microscopy.

The thick sections of cortex were photographed, and a montage encompassing a segment of the entire width of a cortical mantle was prepared. The montages were analyzed for the width of the cortex and for the average density of neurons, glia, and blood vessels per area of cortex. All nuclei not related to either neuron or blood vessels were identified as glia. All identifiable vascular structures, irrespective of their size, were categorized as blood vessels.

The analysis of a cortical montage is limited in that it is only a qualitative assessment. It does not yield the number of structures or the size of a structure. Stereologic procedures are available for light and electron microscopic studies which provide a morphometric analysis of neurons, neuropil, and terminal boutons. The basis for these stereologic procedures and the arguments for their validity have been presented by Weibel (*13*). The relative size of the neurons in the control and lead-intoxicated rats was estimated by comparing comparable neuronal nuclei. The pyramidal neurons in layer V were identified, long and short axes of their nuclei were measured with an eyepiece micrometer, and their areas were calculated from the measured major and minor axes. The numercal density of neurons, the number of neurons per unit volume of cortex, was determined by the method of Weibel and Gomez (*14*). This study was done at the light microscopic level and used the 0.5 μ thick Araldite sections. The volume density of neuropil, the volume of neuropil per unit volume of cerebral cortex, was determined by the point-count method (*13*). Again, this was a light microscopic determination based upon the 0.5 μ thick sections.

The numerical density of terminal boutons and the surface density of the terminal bouton and of their dense zone were analyzed at the ultrastructural level in the cortical layer I, the cortical layer I being almost entirely neuropil. Random selection of the fields to be studied was obtained by taking an electron photomicrograph from the center of a grid square. If the field to be photographed appeared to contain less than 50% neuropil, it was adjusted. Six adjacent central grid squares were photographed per grid. The plate magnification was 13,000 and was consistently enlarged threefold in printing and the magnification monitored as before. The numerical density of the terminal boutons was determined by the same principles employed for the neuronal density (*14*). By assuming that the boutons were elipses presenting oval profiles in section, the long and short axes were measured and the ratio obtained. The criteria used to define terminal boutons were the presence in a membranous profile of three or more small membrane-bound vesicles and the presence of an electron-dense specialized apposing membrane at the junction of a cell process. The average size of terminal bouton was computed by dividing the volume density of terminal boutons by the numerical density. The surface density of the terminal boutons and their specialized electron dense zones were determined by the procedures of Weibel (*13*). The surface density is a ratio between the surface of a bouton and a unit volume of neuropil. The average surface area of a single terminal bouton or its electron-dense line was calculated by dividing the surface density by the numerical density of the terminal boutons.

The size distribution of the cellular processes in the neuropil was analyzed from the electron photomicrographs. A line was drawn across a print and the maximum diameter of all processes subtended by the line was measured.

The results of the light and electron microscopic morphometric studies were combined for each rat, four thick sections and 24 electron micrographs, and the average for the control and the lead-intoxicated groups determined. The significance of the differences between the groups was analyzed by Student's t test (*11*).

Biochemical Analyses

Single brains were employed for most studies, but pools of two to four brains were

necessary for the sphingolipid fatty acid analyses and the fractionation studies. The animals were sacrificed by decapitation, and the brains were removed and weighed. The specimens were generally analyzed immediately; however, a few specimens were stored at −20°C for less than 1 month prior to analysis. Lead determinations were made of homogenized whole brains by the method of Bessman and Layne (*15*). Lipids were extracted by the method of Folch-Pi, Lees, and Sloane-Stanley (*16*). Phospholipid was determined by the procedure of Fiske and Subbarow (*17*). Individual phospholipids were resolved by thin-layer chromatography (TLC) (*18*) with Silica Gel H and quantitated by phosphorus content (*19*). Cholesterol was determined by using the method of Sperry and Brand (*20*), and cerebrosides and sulfatides by the orcinol reaction (*21*). Protein and DNA were extracted from the brain tissue (*22*) and measured by the methods of Lowry et al. (*23*) and Burton (*24*), respectively. Gangliosides were extracted by the method of Suzuki (*25*), resolved into major species by TLC, with Silica Gel H and the neuranimic acid (NANA) content determined by the resorcinol reaction (*26*). Cerebrosides, sulfatides, and ceramides were separated and purified by Florisil column chromatography and TLC with Silica Gel (*27*). These sphingolipids were separated into hydroxy- and *n*-fatty acid-containing species by TLC, cleaved by methanolysis (*28*), and the fatty acid methyl esters extracted into hexane. The composition of these methylated fatty acids was determined by gas-liquid chromatography.

The myelin and synaptosome subfractions were prepared by centrifugation on a discontinuous sucrose-Ficoll gradient as described by Kurokawa et al. (*29*). The purity of the isolated myelin and synaptosome fractions were confirmed by electron microscopy. The gangliosides were extracted as above (*25*), resolved in their major subspecies by TLC with Silica Gel H, and quantified by the resorcinol method (*26*).

Results

The lead-intoxicated rats showed a regular sequence of functional changes (Fig. 1). Between days 22 and 24 there urinary incontinence occurred, and 2–4 days later caudal paraplegia which rapidly evolved over a 24-hr period was noted. If water and the lead-supplemented food were made easily available during this period of disability, many of the paraplegic rats survived to day 30.

The brains of the experimental animals sacrificed on day 30 showed the brown discoloration of the cerebellum (Fig. 1). The brains of these lead animals were smaller and paler (Fig. 1) than those of the controls, but otherwise no differences were noted. Histological preparations revealed focal hemorrhages in the cerebellar folia with endothelial proliferation of small blood vessels and cysts in the medullary cores. The cysts did not have a lining and were surrounded by reactive astrocytes and microglia; few gitter cells were noted. In the remaining regions of the brain, rare cysts were found in the corpus callosum. A Luxol Fast Blue stain revealed many well myelinated tracts, and there were no discernible differences between the control and lead-intoxicated rats. Glia in the white matter of both groups were predominantly mature interfascicular oligodendroglia. In multiple representative sections of cerebrum, cortex was well preserved in the experimental rats and the cyto- and the myelo-architecture were comparably developed in both groups.

Morphometric Studies

With electron microscopy structures of the white matter, myelin sheaths, and axons were indistinguishable in experimental and control animals. However, the quantitative analysis of the pyramidal tract revealed a number of significant differences.

The results of the morphometric analysis of the myelin are presented in Table 1. The ratio of myelinated to nonmyelinated axons was essentially the same in lead and control rats, 41% and 43%, respectively. The analy-

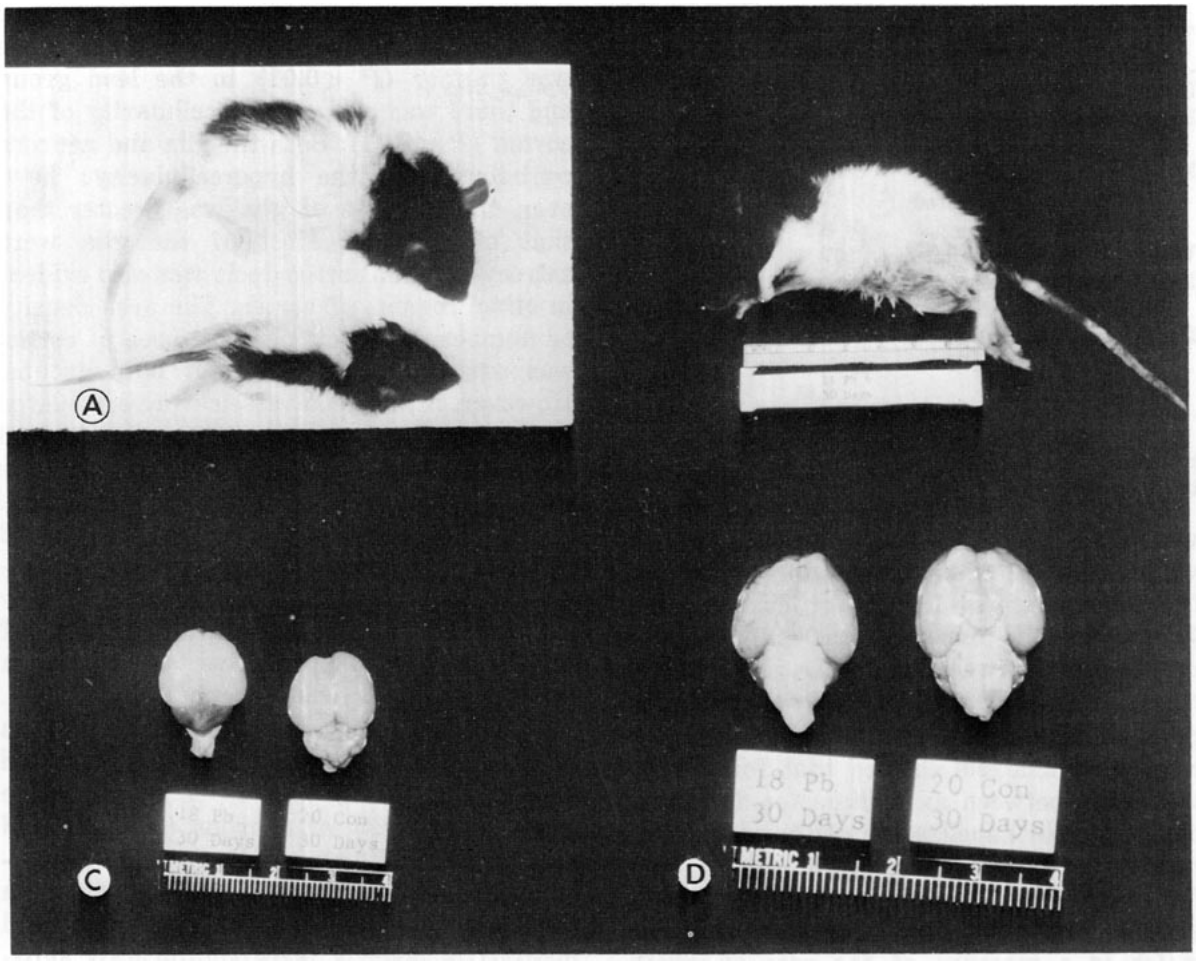

FIGURE 1. Montage of 30-day old control and lead rats: (A) disparity in body size between the control and lead rats; the discoloration of the hind limbs of the lead rat is due to urinary incontinence; (B) photograph showing not only the discoloration due to the incontinence but atrophy of the hind limb musculature; (C) dorsal view of the brains; in the lead rat, the pallor of the cerebral hemispheres and the brown discoloration of the cerebellum are evident; (D) ventral view of the brains; other than the pallor there are no apparent differences.

sis of the number of lamellae in the sheaths of the myelinated axons revealed that there were significantly fewer lamellae ($P < 0.01$) in the experimental animals; the mean for the lead-intoxicated and controls was 7.8 and 8.9 lamellae, respectively. In the axons with but one or two myelin lamellae, the myelin was not compact; these were invariably promyelinating fibers and in both groups comprised less than 0.3% of the myelinated fibers. The regression analysis of the number of myelin lamellae per unit width of the myelin sheath showed that the distance between a single compact myelin lamella, was 107 Å for the controls and 117 Å for the lead-intoxicated rats. This difference was not significant, and the values were comparable to the 106 Å reported by Karlson (*30*) for aldehyde-fixed material. Distribution analysis of the axon size revealed that on the average the axons were larger in the control animals ($P < 0.05$) than in the lead-intoxicated rats. The mean axon circumference was significantly reduced ($P < 0.05$) in the lead rats and the values for control and lead-intoxicated rats

Table 1. Morphometric analysis of myelin and axons of 30-day rats.[a]

	Control	Lead
Unmyelinated fibers, %	43	41
Promyelinating fibers, % of myelinated axons	<0.3	<0.3
Mean number of myelin lamellae per myelinated axon	8.9	7.8
Width of myelin lamella, Å	107	117
Mean diameter of myelinated axons, μ	1.64	1.52
Diameter of axon when initial myelin lamella appears, μ	0.41	0.32

[a] The values are based upon the analysis of the pyramidal tract in the medulla of three lead and three control rats.

were 11.8 and 10.6 units, respectively. If we assume the axon profiles to be circular, the diameters are 1.64 μ for controls and 1.52 μ for the experimental animals. The relationship between axon size and number of myelin lamellae was calculated from the population of axons with 3–20 lamellae. The regression analysis showed that for the relationship between axon diameter and number of myelin lamellae the coefficient of correlation was highly significant ($P < 0.001$) for both the experimental and control groups. The slope of the regression curve, which is a measure of the rate at which the number of myelin lamellae are added per unit increment in axon size, was essentially identical for the two groups. There was a significantly different ($P < 0.05$) value for the axon size on which a compact myelin lamella would theoretically first appear. In the control rat, this was equivalent to a circular axon with a diameter of 0.41 μ while in lead intoxication, the corresponding diameter was 0.32 μ. Myelination was thus initiated on a smaller axon in the lead-intoxicated rat, and the number of myelin lamellae for any given axon diameter was greater in the lead-intoxicated than in the control rats. However, the axons were larger in the control group, and there were more myelin lamellae per brain.

Changes in the cerebral cortex of the lead-intoxicated rats were apparent in all levels of analysis. The results of the analyses of the montages of the somatosensory cortex are presented in Table 2. The cortical mantle was thinner ($P < 0.01$) in the lead group and there was also a hypercellularity of the cortex ($P < 0.01$). Both the glia and neurons contributed to the hypercellularity; however, the increase of glia was greater than that of neurons. Most of the glia were astrocytes. This astrocytosis was also evident in other regions of cortex. The area density or number of vessels per unit area of cortex was essentially the same for both groups. However, if the blood vessels were considered in terms of the neurons, the ratio of blood vessels to neurons was 0.341 and 0.386 for the lead and control groups, respectively. While this decrease in the number of blood vessels per neuron was marginally significant ($0.05 < P < 0.10$), this difference may be important in terms of the observations of an obliteration of selective capillaries in concordance with lead encephalopathy (*31*).

The quantitative morphological analysis of the "thick" plastic sections are presented in Table 3. There was an increase in the numercial density of neurons ($P < 0.05$) ni the lead rats. The neuropil comprised a smaller proportion ($P < 0.05$) of the cortex in the lead rats. The nuclei of the pyramidal neurons in layer V were significantly smaller in the lead rats.

The electron microscopic studies revealed no apparent effects of lead of cortical neuropil development. However, the morphometric analysis of the diameter of the cellular processes in the neuropil brought out an appreciable difference. The cellular processes of the lead-intoxicated rats were larger ($P < 0.01$); the mean diameters were 0.374 and

Table 2. Area density of cells in montages of somatosensory cortex of 30-day rats.

	Control	Lead
Thickness of cortical mantle, mm	1.88	1.56
Cells, mm^{-2}	1107	1623
Glia, mm^{-2}	514	871
Neurons, mm^{-2}	581	685
Blood vessels, mm^{-2}	224	233

Table 3. Quantitative analysis of somatosensory cortex of 30-day rats.

	Control	Lead
Neurons $\times 10^{-4}$ per mm^3	7.05	8.98
Pyramidal neurons, layer V nuclear area, μ^2	78	67
Neuropil, % of cortex	66	57

0.334 μ for the lead and control rats, respectively. In both groups, the synapses analyzed were almost entirely of the axon-dendritic type. The synaptic vesicles were not quantified per bouton examined; however, there were no qualitative differences in the number or the types of vesicles per terminal bouton. All the vesicles were of the hollow spherical type. The morphometric analysis of the terminal boutons (Table 4) revealed no effect of lead intoxication on the numerical density, volume density, or surface density of synapses in the neuropil. There was also no discernible difference in the surface density of the terminal bouton dense line. The values in Table 4 were utilized in calculating the volume, total surface, and dense line surface of an average terminal bouton, and these latter data are presented in Table 5. There were no apparent differences between the lead and the control groups in any of the values obtained for an average bouton.

Chemical Studies:

The general analyses of the brain are summarized in Table 6. Lead concentration was, of course, greater in the lead animals than in the controls, 0.30 ppm and 9.2 ppm, respectively. The DNA concentration normally decreases while the whole brain content of DNA increases during the initial 20–30 postnatal day (*5, 6*). There were no significant differences in DNA content between groups. The DNA concentration was increased, but not significantly, in the lead rats and this probably reflected the increased cellularity of a diffuse gliosis which was apparent in the histological preparations. In addition, the brain protein content was significantly ($P < 0.05$) reduced in the lead rats.

Table 4. Quantitative analysis of synapses in molecular layer of neuropil of somatosensory cortex of 30-day rats.

	Control	Lead
Terminal boutons $\times 10^{-8}$ per mm^3	9.35	10.3
Volume density, mm^3/mm^3	0.156	0.181
Total surface density $\times 10^{-9}$, mm^2/mm^3	3.89	5.12
Dense line surface density $\times 10^{-9}$, mm^2/mm^3	0.871	1.06

Table 5. Morphometric features of an average terminal bouton in molecular layer.

	Control	Lead
Axial ratio	0.66	0.68
Volume, μ^3	0.167	0.175
Total surface, μ^2	4.17	4.96
Dense line surface, μ^2	0.933	1.03

The contents in brain of galactolipids, cholesterol, plasmalogens, and total phospholipids normally rise rapidly during the first 20 postnatal days (*3*). However, by the day 30 (Table 7) the lead-exposed animals had significantly less ($P < 0.02$) of all of these structural lipid constituents. The partition of the phospholipids into their main classes (Table 8) showed no appreciable differences in composition between the experimental and control animals.

Membranes and especially myelin are particularly rich in cerebrosides and sulfatides, as well as the ceramides, which are their likely metabolic precursors. The composition of the fatty acid moieties isolated from these galactolipids (Table 9) showed several features previously reported as indicative of maturing myelin. There is a higher proportion of long-chain hydroxy fatty acids (HFA) than of normal or nonhydroxy fatty acids (NFA) in cerebrosides and sulfatides (*32*). In the ceramides there is a predominance

Table 6. General composition of 30-day rat brains.

	Control	Lead
Lead concn, ppm	0.30	9.2
DNA content, μg	1757	1665
Protein content, mg	164	142
NANA content, μg	1551	1384

Table 7. Lipid composition of 30-day rat brains.

	Control	Lead
Total lipid phosphorus		
Content, μmole	77.6	51.0
Concn, μmole/g wet weight	53.0	43.2
Cholesterol		
Content, μmole	92.8	52.6
Concn, μmole/g wet weight	65.2	43.3
Cerebroside, hexose		
Content, μmole	32.3	21.1
Concn, μmole/g wet weight	22.7	16.1
Plasmalogens		
Content, μmole	25.5	14.4
Concn, μmole/g wet weight	17.2	12.2

of short-chain saturated normal fatty acids (*33*). In these sphingolipids there is a smaller percentage of monounsaturated fatty acids in HFA than in NFA (*20, 27, 34*). The distributions of fatty acid species in the brain cerebrosides and sulfatides of both groups of rats are comparable in general pattern. No unique fatty acids were identified in the lead rats.

The ganglioside content normally increases rapidly during early postnatal life, and a significant difference ($P < 0.01$) was already evident in the experimental group as early as day 30. The gangliosides from whole brain were resolved into major subspecies (Table 10). Neither a significant difference in the whole brain ganglioside composition of the two groups nor an increase in minor gangliosides of the experimental animals was observed. The isolated myelin subfraction reflected a very significant enrichment in G_{M1} as Suzuki has established (*35*). However, no difference in ganglioside composition of myelin from lead-intoxicated and control animals was found. In addition, no differences between the groups were found in the isolated synaptosome fraction.

Discussion

The cerebral growth was impaired in the lead-intoxicated rat. Both the wet weight of brain and the total brain protein were significantly diminished by the 30th postnatal day. On the other hand, the number of cells in the brain as estimated by the DNA content of brain was smaller for both groups. In view of the decreased brain weight and protein content with the preservation of an

Table 8. Composition of phospholipids in brains of lead-intoxicated and control rats.[a]

	Phosphatidyl ethanolamine, %	Phosphatidyl choline, %	Sphingomyelin, %	Phosphatidyl serine + phosphatidyl inositol, %
Control (2)	32.5	36.2	6.1	20.3
Lead (2)	37.0	36.3	5.4	21.6

[a] Phospholipids were obtained from brains of control and lead-intoxicated rats at 30 days postnatal age. The values are expressed as percentage of total lipids. The number of experiments is in parentheses.

Table 9. Selected aspects of fatty acid composition of ceramides, cerebrosides, and sulfatides of control (C) and lead-intoxicated (Pb) rat brain.[a]

	Cerebrosides				Sulfatides				Ceramides	
	Normal fatty acids		α-Hydroxy fatty acids		Normal fatty acids		α-Hydroxy fatty acids		Normal fatty acids	
	C	Pb	C	Pb	C	Pb	C	Pb	C	Pb
Ratio $\frac{22:0-24.0}{16:0-20:0}$	3.0	2.8	20	28	1.6	1.4	20	28	0.2	0.4
Monounsaturated, % of total	41	44	15	16	33	35	18	19	15	19
Total FA, nmole/g wet weight	1088	1013	N	N	687	410	N	N	190	209

[a] Lipids were obtained from brains of control and lead-intoxicated rats at 30 days postnatal age.
N = not detected.

Table 10. Composition of major gangliosides in brains of lead-intoxicated and control rats.[a]

	Whole brain				Myelin subfraction				Synaptosome subfraction			
	^{G}T1	^{G}D1b	^{G}D1a	^{G}M1	^{G}T1	^{G}D1b	^{G}D1a	^{G}M1	^{G}T1	^{G}D1b	^{G}D1a	^{G}M1
Control (8)	19.4	17.9	40.3	22.4	9.4	13.4	27.7	49.5	12.7	12.2	35.1	41.0
Lead (8)	19.3	18.7	39.3	22.7	10.0	13.6	25.2	51.2	11.1	11.9	35.7	45.3

[a] Gangliosides were obtained from brains of control and lead-intoxicated rats at 30-days postnatal age.
Values are expressed as the mole-% of total major gangliosides. The number in parentheses indicates the number of experiments.

apparently normal number of brain cells, we deduce that postnatally lead intoxication leads to restricted cellular growth and retarded maturation (*36*). This is in keeping with our findings of altered cortical development and myelination.

There was a generalized reduction in the mass of gray matter which was most apparent in the cortex. The lead brains weighed less, and the measured cortical mantle was thinner. This reduction in tissue mass was quite complex considering there was actually an increased density of neurons and glia in these gray structures. However, the postnatal cortical ontogenesis of the rat, like other mammals, is one of progressive cortical mantle enlargement secondary to the growth and differentiation of neurons (*37, 38*). Specifically, the neuronal changes consist of growth of soma, dendrites, and axons, a progressive subdivision of axon terminals and of dendrites, and synaptogenesis. In the process of cortical maturation, there is a decrease in the average size of the cell processes constituting the neuropil. This reduction in the size of cellular processes is, as noted above, the result of the subdivision of proximal dendrites into distal twigs and the growth of fine axon sprouts (*38, 39*); thus the larger mean size of the cellular processes noted in the neuropil of the lead rats may be due to a restriction of the subdivision of the axons and the dendrites. A reduction in the subdivision of dendrites and axons in the neuropil readily accounts for part of the reduced cortical growth. It also accounts for the fact that the neuropil constituted a smaller percentage of the cortex in the intoxicated rats than in the control rats. There was also an overall reduction in the size of neuronal nuclei and soma which adds to the overall reduction in cortex. On the basis of a reported constant relationship between neuronal nuclear size and soma size (*40–42*), we are assuming that the homologous neurons were consistently smaller in the lead rats.

In terms of the increased neuronal density, studies by Altman (*6*) and others (*5, 36*) have shown that there is essentially no postnatal neurogenesis in the rat neocortex. It thus appears reasonable to assume there was a stable population of neurons in the lead-intoxicated rats, and the paucity of the neuropil and the overall reduction in neuron size accounts for the increased neuronal density.

In studying the ultrastructure of the neuropil, there were no apparent abnormalities of synaptogenesis. However, a morphometric analysis reveals that the average number of synapses per neuron is reduced. Based upon the results presented in Table 4 this is not evident. The numerical density of synapses was increased in the lead rats; however, this datum is misleading, as it is expressed in terms of neuropil. As also noted in the lead rats (Table 3), the neuropil comprises a smaller proportion of the cortex, and the neuronal density is greater. When the synaptic density was recalculated in terms of cortex and the neuronal density factors are taken into account, the average number of synapses per lead neuron was less ($P < 0.05$) than per control neuron (Table 11).

The basic mechanisms whereby lead intoxication affects synaptogenesis in the developing rat were not apparent. However, on another level, the effect of lead was in the reduction of the available dendritic sites and/or terminal boutons. As has been noted, the lead neurons are relatively smaller than the control neurons. In the cortex, the direct relationship between neuronal size and the extent of dendritic branching has been demonstrated by Bok (*43*). Moreover, based upon the inverse relationship between size of neurite processes in the neuropil and the progressive subdivision of the dendrites and axons, we have further evidence for a reduction in the size of the dendritic tree. In addition, Valverde (*44*) has pointed out that the further a dendritic twig is from the soma, the greater is the density of dendritic

Table 11. Synaptic–neuronal relationship in cortex.

	Control	Lead
Synaptic density in cortex $\times 10^{-5}$ per mm^3	6.17	5.81
Synapses per neuron $\times 10^{-3}$	8.75	6.46

spines per unit length of dendrite. This further emphasizes the significance of the restricted dendritic field in reducing the average number of synapses per neuron. However, the neuropil analysis also suggests that axon subdivision was also retarded. Whether the latter reflects a primary inhibition of proliferation of axon terminals or an inhibition secondary to the absence of dendritic sties is not clear at this time.

By 30 days of age, the lead-intoxicated rats also had a generalized reduction in myelin. While this was not apparent in the histologic preparation, even with myelin stains, there was a significant reduction in brain content of the constituents of membranes (phospholipids, galactolipids, plasmalogens, and cholesterol). The decrease of myelin content was also consistent with the observed decrease in the mean size of an axon plus the decrease in the mean number of myeline lamellae per axon in the lead rats. Quantitatively the decreases of galactolipids and cholesterol were of a similar magnitude for those compounds in which myelin is enriched (*45–47*). The gangliosides, which are concentrated in neurons (*48, 49*), were similarly decreased. A study of the molecular subspecies of the brain phospholipids and gangliosides did not reveal any apparent changes in their composition. The same was true for the detailed ganglioside analysis of the myelin subfraction. All these data suggest that the myelin deficiencies reflect a selective disorder of cellular metabolism. Similarly, the fatty acid analyses of the isolated cerebrosides and sulfatides indicate there was no molecular variation in the myelin membrane of the lead rats. In the same way, our ultrastructural studies showed that the myelin formed in the face of lead intoxication was morphologically indistinguishable from that of the normal rat. Moreover, the relationship between myelination and axon diameter was preserved. While the axons were smaller in the lead rats and myelination added to the axon was initiated on a smaller axon, there was no difference in the percentage of myelinated fibers or of fibers undergoing myelination.

When exposed to excessive dietary lead during postnatal brain development, which includes active myelination and neuronal maturation, the brain of the rat manifested significant deficiencies in myelin lipids and gangliosides. From a temporal study of myelination (*9*), we know that the deficit of ganglioside content occurred prior to the period of most active myelination in the rat and thus preceded the age at which the reduction of myelin lipid content was most apparent. Clearly the neuron and most likely the myelinating glial cell were compromised by the exposure to this heavy metal. We believe it is reasonable to suggest that the decreased myelination represents a secondary hypomyelination following retarded neuronal growth and maturation. Furthermore, while the average axon size was decreased in the lead-poisoned rat, there was a normal investment of myelin lamellae for a given size. This suggests that the initiation and timing of myelination were not significantly affected, though the total proliferation of this membrane was reduced.

REFERENCES

1. Lin-Fu, J. S. Undue absorption of lead among children: A new look at an old problem. N. Engl. J. Med. 286: 702 (1972).
2. David, O., Clark, J., and Voeller, K. Lead and hyperactivity. Lancet (2): 900 (1972).
3. Davison, A. N., and Dobbing, J. The developing brain. In: Applied Neurochemistry. A. N. Davis, and J. Dobbing, Eds. F. A. Davis Co., Philadelphia, 1968.
4. Pentschew, A., and Garro, F. Lead encephalomyelopathy of the suckling rat and its implications of the porphyrinopathic nervous diseases. With special reference to the permeability disorders of the nervous system's capillaries. Acta Neuropathol. (Berlin), 6: 266 (1966).
5. Davison, A. N., and Dobbing, J. Myelination as a vulnerable period in brain development. Brit. Med. Bull. 22: 40 (1966).
6. Altman, J., and Gopal, D. D. Autoradiographic and histological studies of postnatal neurogenesis. 1. A longitudinal investigation of the kinetics, migration and transformation of cells incorporating tritiated thymidine in neonate rats, with special reference to postnatal neurogenesis in some brain regions. J. Comp. Neurol. 126: 337 (1966).
7. Cragg, B. G. The density of synapses and neu-

rons in the motor and visual areas of the cerebral cortex. J. Anat. 101: 639 (1967).
8. Armstrong-Jones, M., and Johnson, R. Quantitative studies of postnatal changes in synapses in rat superficial motor cortex. An electron microscopical study. Z. Zellforsch. Mikrosk. Anat. 110: 559 (1970).
9. Krigman, M. R., et al. Lead encephalopathy in the developing rat: effect upon myelination. J. Neuropathol. Exptl. Neurol. 33: 1 (1974).
10. Krigman, M. R., et al. Lead encephalopathy in the developing rat: Effect upon cortical development. J. Neuropathol. Exptl. Neurol., in press.
11. Dixon, W. J., and Massey, F. J. Introduction to Statistical Analysis. McGraw-Hill, New York, 2nd ed., 1957.
12. Krieg, W. J. S. Connections of the cerebral cortex I. The albino rat. A. Topography of the cortical areas. J. Comp. Neurol. 84: 221 (1946).
13. Weibel, E. R. Stereological principles for morphometry in electron microscopic cytology. Internat. Rev. Cytol. 26: 235 (1969).
14. Weibel, E. R., and Gomez, D. M. A principle for counting tissue structures on random sections. J. Appl. Physiol. 17: 343 (1962).
15. Bessman, S. P., and Layne, E. C., Jr. A rapid procedure for the determination of lead in blood or urine in the presence of organic chelating agents. J. Lab. Clin. Med. 45: 159 (1955).
16. Folch, J., Lees, M., and SloaneStanley, G. H. A simple method for the isolation and purification of total lipides from animal tissues. J. Biol. Chem. 226: 497 (1957).
17. Fiske, C. H., and Subbarow, Y. The colorimetric determination of phosphorus. J. Biol. Chem. 66: 375 (1925).
18. Muldner, H. G., Wherrett, J. R., and Cumings, J. N. Some applications of thin-layer chromatography in the study of cerebral lipids. J. Neurochem. 9: 607 (1962).
19. Bartlett, G. R. Phosphorus assay in column chromatography. J. Biol. Chem. 234: 466 (1959).
20. Sperry, W. M., and Brand, F. C. The colorimetric determination of cholesterol. J. Biol. Chem. 150: 315 (1943).
21. Hess, H. H., and Lewin, E. Microassay of biochemical structural components in nervous tissue. II. Methods for cerebrosides, proteolipid proteins and residue proteins. J. Neurochem. 12: 205 (1965).
22. Schneider, W. C. Determination of nucleic acids in tissues by pentose analysis. In: Methods in Enzymology, S. P. Colowick and N. O. Kaplan, Eds. Academic Press, New York, Vol. III, 1957, p. 680.
23. Lowry, O. H., et al. Protein measurement with the Folin phenol reagent. J. Biol. Chem. 193: 265 (1951).
24. Burton, K. Determination of DNA concentration. In: Methods in Enzymology, L. Grossman and K. Moldane, Eds. Academic Press, New York, Vol. XII, Part B, 1968, p. 163.
25. Suzuki, K. A simple and accurate micromethod for quantitative determination of ganglioside patterns. Life Sci. 3: 1227 (1964).
26. MacMillan, V. H., and Wherrett, J. R. A modified procedure for the analysis of mixtures of tissue gangliosides. J. Neurochem. 16: 1621 (1969).
27. Joseph, K. C., and Hogan, E. L. Fatty acid composition of cerebrosides, sulphatides and ceramides in murine sudanophilic leucodystrophy: The Jimpy mutant. J. Neurochem. 18: 1639 (1971).
28. Morrison, W. R., and Smith, L. M. Preparation of fatty acid methyl esters and dimethylacetals from lipids with boron fluoride–methanol. J. Lipid Res. 5: 600 (1964).
29. Kurokawa, M., Sakamoto, T., and Kato, M. Distribution of sodium-plus-potassium-stimulated adenosine-triphosphatase activity in isolated nerve ending particles. Biochem. J. 97: 833 (1965).
30. Karlsson, U. Comparison of the myelin period of peripheral and central origin by electron microscopy. J. Ultrastruct. Res. 15: 451 (1966).
31. Rosenblum, W. I., and Johnson, M. G. Neuropathologic changes produced in suckling mice by adding lead to the maternal diet. Arch. Pathol. 85: 640 (1968).
32. Kishimoto, Y., and Radin, N. S. Composition of cerebroside acids as a function of age. J. Lipid Res. 1: 79 (1959–1960).
33. O'Brien, J. S., and Sampson, E. L. Fatty acid and fatty aldehyde composition of the major brain lipids in normal human brain gray matter, white matter and myelin. J. Lipid Res. 6: 545 (1965).
34. Joseph, K. C., et al. Fatty acid composition of cerebrosides, sulphatides and ceramides in murine leucodystrophy: The Quaking mutant. J. Neurochem. 19: 307 (1972).
35. Suzuki, K., Poduslo, S. E., and Norton, W. T. Gangliosides in the myelin fraction of developing brains. Biochem. Biophys. Acta 144: 375 (1967).
36. Winick, M. Nutrition and nerve cell growth. Fed. Proc. 29: 1510 (1970).
37. Caley, D. W., and Maxwell, D. S. Development of the blood vessels and extracellular spaces during postnatal maturation of rat cerebral cortex. J. Comp. Neurol. 138: 31 (1970).
38. Voeller, K. Pappas, G. D., and Purpura, D. P. Electron microscope study of development of cat superficial neocortex Exp. Neurol. 7: 107 (1963).
39. Meller, K., Breipohl, W., and Glees, P. Synaptic organization of the molecular layer in the motor cortex in the white mouse during postnatal

development. A Golgi- and electron microscopical study. Z. Zellforsch. Mikrosk. Anat. 92: 217 (1968).

40. Bok, S. T. A quantitative analysis of the structure of the cerebral cortex. Proc. Acad. Sci. Amster. 35: 1 (1936).
41. Donaldson, H. H., and Nagasaka, G. On the increase in the diameters of nerve-cell bodies and of the fibers arising from them during the later phases of growth (albino rat). J. Comp. Neurol. 29: 529 (1918).
42. Hertwig, O. Über Korrelation von Zell und Kerngrösse and ihre Bedeutung für die geschlechtliche Differentzierung und die Teilung der Zelle. Biol. Zentr. 23: 49 (1903).
43. Bok, S. T. The branching of dendrites in the cerebral cortex. Proc. Acad. Sci. Amster. 39: 1209 (1936).
44. Valverde, F. Apical dendritic spines of the visual cortex and light deprivation in the mouse. Exper. Brain Res. 3: 337 (1967).
45. Brante, G. Studies on lipids in the central nervous system. With special reference to quantitative chemical determination and topical distribution. Acta Physiol. Scand. 18 (Suppl. 63): 1 (1949).
46. Folch-Pi, J., et al. Chemistry of myelin development. In: The Biology of Myelin, S. Korey, Ed. Hoeber-Harper, New York, 1959.
47. Norton, W. T., and Autilo, L. A. The lipid composition of purified bovine brain myelin. J. Neurochem. 13: 213 (1966).
48. Kishimoto, Y., et al. Gangliosides and glycerophospholipids in multiple sclerosis white matter. Arch. Neurol. 16: 44 (1967).
49. Lowden, J. A., and Wolfe, L. S. Studies on brain gangliosides. III. Evidence for the location of gangliosides specifically in neurons. Can. J. Biochem. 42: 1587 (1964).